

Chapter 3

Investigation of the Eigen Frequency of a Cantilever Microbeam Immersed in a Fluid under the Piezoelectric Effect

V. Elias, F. Braud, P. Champagne and G. Nassar

3.1. Introduction

The Micro Electromechanical systems (MEMS) use micro-sized components for sensors, transducers, actuators, and electronic. The MEMS appeared in the 1960s, were quickly integrated into electronic products, they appeared with the arrival of microelectronic technologies, and cantilever microbeams are sensors from this MEMS family. The first uses of vibrating cantilevers microbeam for mass detection date back to the 1980s. In 1994, Gimzewski et al. [1] developed a new form of calorimeter based on microcantilever which can sense chemical reaction.

In our day, the cantilever microbeams are frequently used to detected biological and chemical microparticles [2-10], to probe viscosity and density of gases and liquids replacing rheometer [11-18] or to detect changes in mass, stress or temperature [19-22]. Wide historical studies have been released on the vibrational microbeam immersed in a fluid [23-25] and many profound theoretical models were done to explain the behavior of the fluid environment and they were ascertained after that by experimental measurements [26-28]. Lately, advanced studies were done by G. Brunetti et al. for the detection of multiple target molecules [29] and with J. Duffy et al. miRNA for the detection of cancer [30] in serum samples.

The process of the system introduces a vibration on the microbeam immersed in a fluid with exciting it periodically by a piezoelectric effect. It is necessary to find the link between the physical parameters of the modification of the natural frequency when the micro-beam is in vibration mode with different surroundings parameters, this linkage helps us in our study. Commonly, two ways of measuring the detection mode are available: by deflection in static mode [31, 32] or by shifting resonance in dynamic mode [7, 33].

Generally, many of these applications have been recently developed and used as a very sensitive detector of heat, surface stress, mass or in molecular recognition conducted in a fluid surroundings (gas or liquid). This new model is necessary because it makes progress about detection of gas or humidity in gaseous medium. On the other hand, in liquid medium, they are mainly used for the detection of specific biological molecules (antigen / antibody reactions). The cantilevers microbeam used in the biomedical field are called BioMEMS and this device have become the largest and most diverse applications of MEMS devices. Therefore, it is important to consider how the density of the fluid and the additional mass on the beam affect the behavior of the natural frequency. In other words, measuring the resonant frequency shift during the cantilever excitation frequency sweep reveals an intruder in the surrounding environment.

In our study we will adopt a new method to excite the system by a short electrical pulse periodically on a piezoelectric element embedded in the mass structure of the device, playing the role of an external source (see Fig. 3.1). Then we will try to estimate the variations in the eigenvalue's resonant frequencies. The aim is to prove that with our new proposal we can reach a cantilever system with a beam thickness of 10 μm which will have a high sensitivity compared to other systems.

3.2. Materials & Methods

Our Methodology begins by using numerical technology and simulating the physical concept with charges effects to illustrate the functional analysis of the results (frequency deviations and electrical signal properties) using a Multiphysics software. Then, the accuracy of the proposed model is validated by close comparison studies of the theoretical calculations to our numerical work using the models of Van Eysden and Sader [34-36].

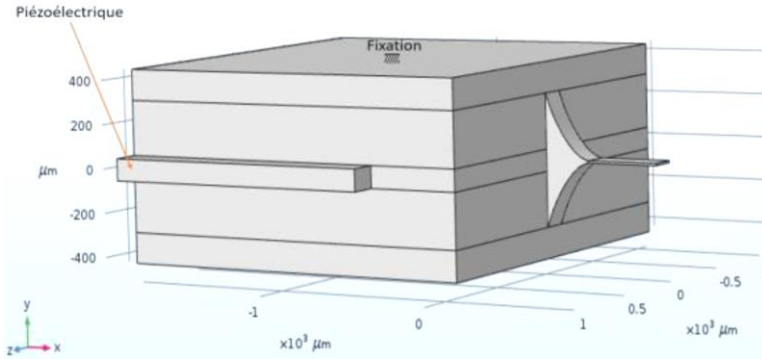


Fig. 3.1. Mechanical Structure of our device.

Several types of excitation are used to make the beam vibrate, the source can be by the effect of electromagnet, thermal noise, or piezoelectric like in our case. Preliminary studies have resulted in the assumption that placing the piezoelectric as a layer under the beam causes the metal to melt at the desired frequencies. Furthermore, this placement also might be causing many reactions with the environment of the experiment since the piezoelectric is in contact with the medium. To avoid these risks, we proposed a new model of structure depicted in Fig. 3.1, that were the piezoelectric with 10 μm of width is sandwiched in a box of silica. And this box is engraved in an exponential shape ended by a thin beam having a length of 400 μm , width of 140 μm and thickness of 10 μm . This design participates in the transfer of stresses from the box to the beam in an efficient way, by reducing the loss and increasing the quality factor. The maximum frequency of the peak depends on the mass and the rigidity of the structure.

A periodic pulse excitation signal is generated by an external source on the piezoelectric while only immersing the beam in a chamber volume of 1.76 μL of incompressible fluid. The maximum displacement of the beam represents the fundamental frequency of the system and creates acoustic pressure on the surrounding fluid as depicted in Fig. 3.2.

Any change in the resonant frequency for the next pulse is a function of the change in the environmental characteristics, whether it is the mass of viral particles attached to the surface of the cantilever beam or a change in fluid density. Unlike other methods of measurement by optical reflection [3], deflection of the actuated cantilever electrode [37],

piezoresistive [38] or shifting in resonance frequency [7], our way of measuring depends on analyzing what can be detected when the voltage pulse goes to 0. A frequency value is read on the piezoelectric, depending on the damping mode caused by the beam that vibrates, in addition to the shifting frequency for two consecutive eigenfrequencies. With this system, installation and nano-wire complicity is reduced. According to a study done by Ghatkesar et al. [39], the peak frequency is notably scattered in function of time as for the eigenfrequencies, they are recorded orderly. These findings drove us to rely on the eigenfrequencies. According to our simulation, the deviation between the peak-frequency and the eigenfrequency is small while increasing in harmonic mode. In these tests, we have found for the order of vibration of the 1st, 2nd, 3rd, 5th and 13th normal mode in a fluid medium in addition to the order vibration of 16th mode in air surrounding, that the beam has an appropriate movement for node fraction, which helps us arriving to the possibility of adsorption on the beam while avoiding the fall of particles from the pores.

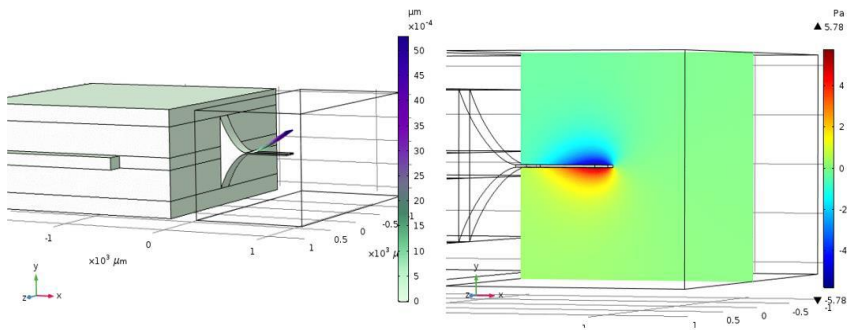


Fig. 3.2. The displacement of the beam for a fundamental frequency (in the left figure), and the acoustic pressure exerted on the beam by the surrounding for a fundamental frequency (in the right figure).

3.3. Results & Discussion

3.3.1. Density and Dynamic Viscosity Test

The micro-cantilever beam is more sensitive to changes in density than in viscosity while using a beam with 1 μm of width according to Ghatkesar et al. [40].

To move towards greater precision in density and viscosity changes we compared the 5th harmonic mode with the 13th harmonic mode by who have the biggest shift in eigen frequency while changing in density and viscosity. while using our exponential model which ends with a beam width of 10 μm . Taking water with 997 Kg/m^{-3} of density and 0.913 of viscosity as a reference to examine the frequency changes and to illustrate the sensation variation between our device of 10 μm of width with other thinner devices. According to our tests done before, as we go up in harmonic mode, there is an increase in the changing frequencies, than with the fluids surrounding tests in this chapter, we use the 13th mode as an eigen value.

The eigen frequency f_{0n} is characterized by this equation (3.1) in the absence of damping with:

$$f_{0n} = \frac{\alpha_n^2}{2\pi} \sqrt{\frac{k}{3(m_c+m_l)}}, \quad (3.1)$$

where α_n are related to the different eigenvalues of the harmonics [41], m_c is the mass of cantilever, m_l is the virtual mass of the liquid, k is the spring constant given by $k = 3 \frac{EI}{L^3}$ where EI is the flexural rigidity, with E Young's modulus and I the moment of inertia and L is the length of the cantilever. The peak frequency f_n is characterized by this equation (3.2) in the presence of damping with:

$$f_n = \sqrt{f_{0n}^2 - \frac{\gamma^2}{2\pi}}, \quad (3.2)$$

where the damping factor γ is defined by:

$$\gamma = \frac{c_0+c_v}{\left(\frac{2}{L}\right)(m_c+m_l)}, \quad (3.3)$$

where c_v is the dissipation coefficient, c_0 is the intrinsic damping coefficient per unit length that describes internal losses.

In 5 % of glycerol test and 5 % of ethylene glycol test we inferred that the viscosity is constant, per contra in 5 % of glycerol test and 12 % of ethylene glycol the density is constant. These tests in Fig. 3.3 are carried out to make a comparison between the density and the viscosity at the level of frequency sensitivity.

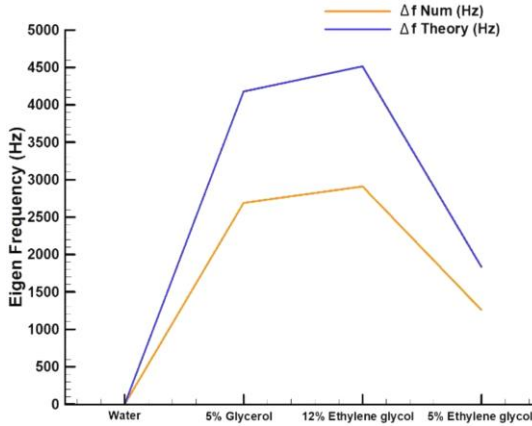


Fig. 3.3. Theoretical and numerical shifts eigen frequency were calculated according to [35] at mode 13th.

As we can see in the Fig. 3.3, in 5 % of glycerol, the numerical eigenfrequencies shifted in the center of 680 kHz by -2690 Hz, in 12 % of ethylene glycol, it shifted by -2910 Hz and in 5 % of ethylene glycol, it shifted by -1260 Hz.

Correspondingly, in 5 % of glycerol, the analytical eigenfrequencies shifted in the 13th mode by -4178 Hz, in 12 % of ethylene glycol, it shifted by -4514.6 Hz and in 5 % of ethylene glycol, it shifted by -1833.8 Hz.

We have noticed that the change in density is 0.055 % and the change in viscosity is 4.41 %.

Our findings suggest that the beam thickness used with this model has better density sensitivity than previous models.

3.3.2. Adsorption Particles

Potassium is a chemical element that exists in the form of an ion in the body. It is present in the serum and too much or too little potassium in the blood plasma can lead to cardiac complications. The normal value of the potassium level should be between 3.5 and 5 mmol/L, of all human beings. A decrease in potassium levels called "hypokalemia" (<3.5 mmol/L) often caused by digestive problems, can cause fatigue, muscle cramps [42]. Too much potassium in the blood is called

"hyperkalemia" (> 4.5 mmol/L) and can cause serious heart problems, which can lead to cardiac arrest and death without emergency chelation therapy. Several studies on the cardiac disease are done to detect a specific marker in serum the C-reactive protein for this pathology [3]. In fact, our model is based on the density variation caused by the potassium rate. The potassium level in mmol/L can affect the serum density in kg/m^3 according to this equation $C_m = CM \times MM$ where C_m is mass concentration in g/L, CM is molar concentration in mol/L and MM is the potassium molar mass, equals to 39.1 g/mol.

We took a serum density of 1024.136 kg/m^3 as an arbitrary value for a normal patient as an example, who have an eigen frequency between 640510 Hz and 640530 Hz.

The density increases while increasing the amount of potassium and decreases while decreasing the amount of potassium as shown in Table 3.1.

Table 3.1. Showing the effect of potassium rate (in mmol/L and g/L) on the liquid density, and displaying the variation in density with that of the frequency in the 13th mode.

Total Density Kg/m^3	1024.0	1024.039	1024.078	1024.117	1024.136	1024.176	1024.19	1024.23	1024.27	1024.31	1024.35	1024.39
Potassium Rate g/L	0	0.039	0.078	0.117	0.136	0.176	0.19	0.23	0.27	0.31	0.35	0.39
Potassium Rate mmol/L	0	1	2	3	3.5	4.5	5	6	7	8	9	10
Mode 13th Hz	640600	640580	640560	640540	640530	640510	640500	640490	640490	640480	640470	640460

The frequency shift is from 640510 Hz to 640460 Hz with 0.254 g/L of density for hyperkalemia disease (> 5 mmol/L) and from 640530 Hz to 640400 Hz with -0.136 g/L of density for hypokalemia disease (< 3 mmol/L) insofar as shown in Fig. 3.4. We have noticed that the change is $20 \text{ Hz/mmol.L}^{-1}$.

By examining the curve shown in Fig. 3.4, it can be noticed that the change in frequency is shifted by 140 Hz in a change of 0.39 g/L of potassium. Moreover, the SiO_2 is a porous material where the average pore diameter is between 2.6 and 68.3 nm [43] compatible with the diameter of potassium particles of 550 pm. Based on the aforementioned,

it is possible that these potassium beads are adsorbed on the beam during the vibration, and this will be a great incentive to change the eigen frequency.

The validation was done using COMSOL Multiphysics software as depicted in Fig. 3.5 with the red beads being the potassium particles and the bleu lines being the beam clamped on one edge. The change in the eigen frequency as a function of the mass of particles attached to the surface of the cantilever beam constitutes could be the basis of the detection scheme.

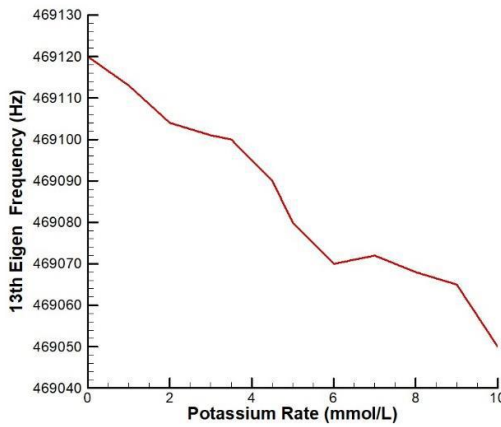


Fig. 3.4. Variation of the 13th natural frequency mode with the potassium level and indicate the range of the patient hypokalemia, normal and hyperkalemia.

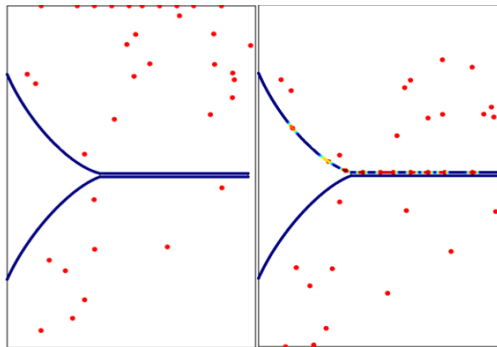


Fig. 3.5. Potassium adsorption on the surface of SiO₂ beam.

3.3.3. Added Mass

For an additional optimization, we made several numerical estimations of Δf variation for two different methods of added masses on the beam as shown in Fig. 3.6.

For the accuracy, this test is validated by a close comparison of the studies of the theoretical calculations with our numerical works by using this equation:

$$f_{0n} = \frac{\alpha_n^2}{2\pi} \sqrt{\frac{k}{3(m_c + m_l + \Delta_m)}}, \quad (3.4)$$

where Δ_m is related to the loaded mass distributed on the surface of the cantilever and the eigen frequency f_{0n} is characterized by this equation (3.4) in the absence of damping.

As shown in Fig. 3.6, the first test was at the center of 640 KHz (13th Mode) surrounded by a fluid and the mass was added on the whole surface with an accuracy of 90 Hz/ng. The second test was at the center of 961 KHz (16th Mode) under vacuum and the mass was added on the whole surface with an accuracy of 390 Hz/ng.

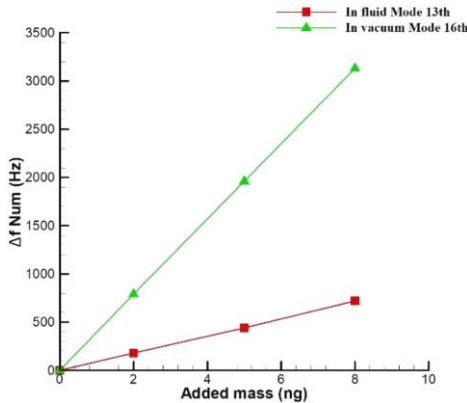


Fig. 3.6. Δf Num in fluid for Mode 13th and in vacuum for Mode 16th.

Our numbers show that in liquid medium the shifting frequency is much more pronounced than in vacuum owing to the influence of hydrodynamic force on the cantilever.

3.4. Conclusions & Outlook

According to our findings, this new microcantilevers shape have been designed to analyze their sensitivity in a chosen medium and it has proven effective. This device can detect up to 0.055 % density and 4.4 % viscosity changes, measured in a chamber volume of 1.76 μL in mode 13th. Consequently, it can diagnose the patient's disease based on the frequency change caused by the potassium level present in the serum by a precision of 20 Hz/ mmol.L^{-1} . Furthermore, this device can detect a small added mass in vacuum by an accuracy of 390 Hz/ng with mode 16th and in fluid by an accuracy if 90 Hz/ng with mode 13th. However, we should ascertain our data with the experimental part using physical realization by laser engraving on SiO_2 support and integrating the excitation source in the overall structure. Then we should verify these values by the analytical part.

The target in this study is to pave the way for several biological topics and especially the diseases that have signs in the blood and urine. Detecting cancer before it metastasizes by the detection of trace biological entities in the serum, can save a patient, prevent disease progress, and give possibility of diagnosing the pathology at its very first stage before spreading. Our future goal is to develop a system with arrays of eight silica beam for the early detection of cancerous potential, it makes it possible to identify new genetic and epigenetic biomarkers linked to any cancer present in the blood, and to find a specific coated cantilever for each disease. This chapter could be interesting for several research where we can use the analyzing natural frequency shift as a sign for a disease by studying the rheological serum properties.

References

- [1]. J. K. Gimzewski, Ch. Gerber, E. Meyer, R. R. Schlittler, Observation of a chemical reaction using a micromechanical sensor, *Chemical Physics Letters*, Vol. 217, Issue 5, 1994, pp. 589-594.
- [2]. H. Lang, et al., A chemical sensor based on a micromechanical cantilever array for the identification of gases and vapors, *Applied Physics A*, Vol. 66, 1998, pp. S61-S64.
- [3]. C.-H. Chen, et al., A wireless bio-MEMS sensor for C-reactive protein detection based on nanomechanics, *IEEE Transactions on Biomedical Engineering*, Vol. 56, 2009, pp. 462-470.
- [4]. I. Dufour, D. Rebiere, F. Lochon, Détection de COV: Des microcapteurs à base de micropoutres, *Info Chimie Magazine*, Vol. 468, 2006, pp. 66-69.

- [5]. F. Huber, H. Lang, N. Backmann, D. Rimoldi, C. Gerber, Direct detection of a BRAF mutation in total RNA from melanoma cells using cantilever arrays, *Nature Nanotechnology*, Vol. 8, 2013, pp. 125-129.
- [6]. K. Hwang, J. H. Lee, J. Park, D. Yoon, J. Park, T. Kim, In-situ quantitative analysis of a prostate-specific antigen (PSA) using a nanomechanical PZT cantilever, *Lab on a Chip*, Vol. 4, 2005, pp. 547-552.
- [7]. J. H. Lee, K. S. Hwang, J. Park, K. H. Yoon, D. S. Yoon, T. S. Kim, Immunoassay of prostate-specific antigen (PSA) using resonant frequency shift of piezoelectric nanomechanical microcantilever, *Biosensors and Bioelectronics*, Vol. 20, Issue 10, 2005, pp. 2157-2162.
- [8]. X. Zhou, S. Wu, H. Liu, X. Wu, Q. Zhang, Nanomechanical label-free detection of aflatoxin B1 using a microcantilever, *Sensors and Actuators B: Chemical*, Vol. 226, 2015, pp. 24-29.
- [9]. W. Zhou, A. Khaliq, Y. Tang, H. Ji, R. R. Selmic, Simulation and design of piezoelectric microcantilever chemical sensors, *Sensors and Actuators A: Physical*, Vol. 125, Issue 1, 2005, pp. 69-75.
- [10]. A. Gupta, D. Akin, R. Bashir, Single virus particle mass detection using microresonators with nanoscale thickness, *Appl. Phys. Lett.*, Vol. 84, Issue 11, 2004, pp. 1976-1978.
- [11]. N. Belmiloud, I. Dufour, L. Nicu, A. Colin, J. Pistre, Vibrating Microcantilever used as Viscometer and Microrheometer, in *Proceedings of the IEEE SENSORS*, 2006, pp. 753-756.
- [12]. W. Shih, X. Li, H. Gu, W.-H. Shih, I. Aksay, Simultaneous liquid viscosity and density determination with piezoelectric unimorph cantilevers, *Journal of Applied Physics*, Vol. 89, 2001, 1497.
- [13]. N. Belmiloud, I. Dufour, A. Colin, L. Nicu, Rheological behavior probed by vibrating microcantilevers, *Appl. Phys. Lett.*, Vol. 92, Issue 4, 2008, 041907.
- [14]. S. Boskovic, J. W. M. Chon, P. Mulvaney, J. E. Sader, Rheological measurements using microcantilevers, *Journal of Rheology*, Vol. 46, Issue 4, 2002, pp. 891-899.
- [15]. D. Kim, S. Hong, J. Jang, J. Park, Determination of fluid density and viscosity by analyzing flexural wave propagations on the vibrating microcantilever, *Sensors*, Vol. 17, 2017, 2466.
- [16]. M. Youssry, N. Belmiloud, B. Caillard, C. Ayela, C. Pellet, I. Dufour, A straightforward determination of fluid viscosity and density using microcantilevers: Analytical and experimental studies, *Procedia Engineering*, Vol. 5, 2010, pp. 1035-1038.
- [17]. M. Hennemeyer, S. Burghardt, R. W. Stark, Cantilever micro-rheometer for the characterization of sugar solutions, *Sensors (Basel)*, Vol. 8, Issue 1, 2008, pp. 10-22.
- [18]. A. Quist, A. Chand, S. Ramachandran, D. Cohen, R. Lal, Piezoresistive cantilever based nanoflow and viscosity sensor for microchannels, *Lab on Chip*, Vol. 6, Issue 11, 2006, pp. 1450-1454.

- [19]. M. Toda, N. Inomata, T. Ono, I. Voiculescu, Cantilever beam temperature sensors for biological applications, *IEEE Transactions on Electrical and Electronic Engineering*, Vol. 12, Issue 2, 2017, pp. 153-160.
- [20]. N. V. Lavrik, M. J. Sepaniak, P. G. Datskos, Cantilever transducers as a platform for chemical and biological sensors, *Review of Scientific Instruments*, Vol. 75, Issue 7, 2004, pp. 2229-2253.
- [21]. I. Voiculescu, F. Liu, T. Ono, M. Toda, Investigation of bimaterial cantilever beam for heat sensing in liquid, *Sensors and Actuators A: Physical*, Vol. 242, 2016, pp. 58-66.
- [22]. T. Thundat, R. J. Warmack, G. Y. Chen, D. P. Allison, Thermal and ambient-induced deflections of scanning force microscope cantilevers, *Appl. Phys. Lett.*, Vol. 64, Issue 21, 1994, pp. 2894-2896.
- [23]. J. E. Sader, Frequency response of cantilever beams immersed in viscous fluids with applications to the atomic force microscope, *Journal of Applied Physics*, Vol. 84, Issue 1, 1998, pp. 64-76.
- [24]. R. Berger, Ch. Gerber, H. P. Lang, J. K. Gimzewski, Micromechanics: A toolbox for femtoscale science: "Towards a laboratory on a tip", *Microelectronic Engineering*, Vol. 35, Issue 1, 1997, pp. 373-379.
- [25]. C.-C. Liang, C.-C. Liao, Y.-S. Tai, W.-H. Lai, The free vibration analysis of submerged cantilever plates, *Ocean Engineering*, Vol. 28, Issue 9, 2001, pp. 1225-1245.
- [26]. W. Lin, N. Qiao, Vibration and stability of an axially moving beam immersed in fluid, *International Journal of Solids and Structures*, Vol. 45, Issue 5, 2008, pp. 1445-1457.
- [27]. M. Aureli, M. Porfiri, Low frequency and large amplitude oscillations of cantilevers in viscous fluids, *Appl. Phys. Lett.*, Vol. 96, Issue 16, 2010, 164102.
- [28]. E. Grimaldi, M. Porfiri, L. Soria, Finite amplitude vibrations of a sharp-edged beam immersed in a viscous fluid near a solid surface, *Journal of Applied Physics*, Vol. 112, Issue 10, 2012, 104907.
- [29]. G. Brunetti, et al., Nanotechnological immunoassay for rapid label-free analysis of candidate malaria vaccines, *Nanoscale*, Vol. 13, 2021, pp. 2338-2349.
- [30]. J. Duffy, F. Padovani, G. Brunetti, P. Noy, U. Certa, M. Hegner, Towards personalised rapid label free miRNA detection for cancer and liver injury diagnostics in cell lysates and blood based samples, *Nanoscale*, Vol. 10, 2018, pp. 12797-12804.
- [31]. G. Thakur, K. Jiang, D. Lee, K. Prashanthi, S. Kim, T. Thundat, Investigation of pH-induced protein conformation changes by nanomechanical deflection, *Langmuir*, Vol. 30, Issue 8, 2014, pp. 2109-2116.
- [32]. K. Jiang, et al., Rapid and highly sensitive detection of dopamine using conjugated oxaborole-based polymer and glycopolymer systems, *ACS Appl. Mater. Interfaces*, Vol. 9, Issue 18, 2017, pp. 15225-15231.

- [33]. J. Joo, D. Kwon, C. Yim, S. Jeon, Highly sensitive diagnostic assay for the detection of protein biomarkers using microresonators and multifunctional nanoparticles, *ACS Nano*, Vol. 6, 2012, pp. 4375-4381.
- [34]. C. A. Van Eysden, J. E. Sader, Resonant frequencies of a rectangular cantilever beam immersed in a fluid, *Journal of Applied Physics*, Vol. 100, Issue 11, 2006, 114916.
- [35]. C. A. Van Eysden, J. E. Sader, Frequency response of cantilever beams immersed in viscous fluids with applications to the atomic force microscope: Arbitrary mode order, *Journal of Applied Physics*, Vol. 101, Issue 4, 2007, 044908.
- [36]. C. A. Van Eysden, J. E. Sader, Frequency response of cantilever beams immersed in compressible fluids with applications to the atomic force microscope, *Journal of Applied Physics*, Vol. 106, Issue 9, 2009, 094904.
- [37]. M. SoltanRezaee, M. Bodaghi, Simulation of an electrically actuated cantilever as a novel biosensor, *Scientific Reports*, Vol. 10, 2020, 3385.
- [38]. K. W. Wee, et al., Novel electrical detection of label-free disease marker proteins using piezoresistive self-sensing micro-cantilevers, *Biosensors and Bioelectronics*, Vol. 20, Issue 10, 2005, pp. 1932-1938.
- [39]. T. Braun, et al., Micromechanical mass sensors for biomolecular detection in a physiological environment, *Physical Review E: Statistical, Nonlinear, and Soft Matter Physics*, Vol. 72, 2005, 031907.
- [40]. M. K. Ghatkesar, E. Rakhmatullina, H.-P. Lang, C. Gerber, M. Hegner, T. Braun, Multi-parameter microcantilever sensor for comprehensive characterization of Newtonian fluids, *Sensors and Actuators B: Chemical*, Vol. 135, Issue 1, 2008, pp. 133-138.
- [41]. P. A. A. Laura, J. L. Pombo, E. A. Susemihl, A note on the vibrations of a clamped-free beam with a mass at the free end, *Journal of Sound and Vibration*, Vol. 37, Issue 2, 1974, pp. 161-168.
- [42]. Potassium: Comprendre son taux lors d'une prise de sang, <https://sante.journaldesfemmes.fr/fiches-anatomie-et-examens/2493150-potassium-comprendre-taux-prise-de-sang/>
- [43]. T. Mochizuki, D. Atong, S.-Y. Chen, M. Toba, Y. Yoshimura, Effect of SiO₂ pore size on catalytic fast pyrolysis of Jatropha residues by using pyrolyzer-GC/MS, *Catalysis Communications*, Vol. 36, 2013, pp. 1-4.